


Theoretical study on $\Lambda_c^+ \rightarrow \Lambda K^+ \bar{K}^0$ decay and $\Xi^*(1690)$ resonance

Si-Wei Liu,^{1,2,*} Qing-Hua Shen^{1,2,†} and Ju-Jun Xie^{1,2,3,‡}

¹*Institute of Modern Physics, Chinese Academy of Sciences, Lanzhou 730000, China*

²*School of Nuclear Sciences and Technology, University of Chinese Academy of Sciences, Beijing 101408, China*

³*Southern Center for Nuclear-Science Theory (SCNT), Institute of Modern Physics, Chinese Academy of Sciences, Huizhou 516000, Guangdong Province, China*

 (Received 21 July 2023; revised 11 October 2023; accepted 9 November 2023; published 11 December 2023)

We present a theoretical study of the $\Xi^*(1690)$ resonance in the $\Lambda_c^+ \rightarrow \Lambda K^+ \bar{K}^0$ decay, where the weak-interaction part proceeds through the Cabibbo-favored process $c \rightarrow s + u\bar{d}$. Next, the intermediate two mesons and one-baryon state can be constructed with a pair of $q\bar{q}$ with the vacuum quantum numbers. Finally, the $\Xi^*(1690)$ is mainly produced from the final-state interactions of $\bar{K}\Lambda$ in coupled channels, and this is shown in the $\bar{K}\Lambda$ invariant mass distribution. The scalar meson $a_0(980)$ and nucleon excited state $N^*(1535)$ are also taken into account in the decaying channels $K^+ \bar{K}^0$ and $K^+ \Lambda$, respectively. Within model parameters, the $K^+ \bar{K}^0$, $\bar{K}^0 \Lambda$, and $K^+ \Lambda$ invariant mass distributions are calculated, and it is found that our theoretical results can well reproduce the experimental measurements, especially for the clear peak around 1690 MeV in the $\bar{K}\Lambda$ spectrum. The proposed weak decay process $\Lambda_c^+ \rightarrow \Lambda K^+ \bar{K}^0$ and the interaction mechanism can provide valuable information on the nature of the $\Xi^*(1690)$ resonance.

DOI: [10.1103/PhysRevD.108.114006](https://doi.org/10.1103/PhysRevD.108.114006)

I. INTRODUCTION

The study of the properties of the Ξ^* states has attracted much attention in hadron physics [1–5]. However, our knowledge about the Ξ spectrum is quite scarce [6]. Except for the ground $\Xi(1321)$ state with spin parity $J^P = 1/2^+$ and $\Xi^*(1530)$ with $J^P = 3/2^+$ being well established with four-star ratings, the situation for other Ξ^* excited states is still rather uncertain with less than three-star ratings [6]. The existence of some of them has not been confirmed. Hence, further studies of the Ξ^* resonances on both the experimental and theoretical sides are necessary [7–10].

For the study of Ξ^* resonances, the $\bar{K}N$ scattering is available [11]. Indeed, the $\Xi^*(1690)$ resonance was first observed in the $\bar{K}\Sigma$ invariant mass spectrum [12] in the K^-p reactions at 4.2 GeV. In the measurements of Ref. [12], the mass and total decay width of $\Xi^*(1690)$ are established as $M = 1694 \pm 6$ MeV and $\Gamma = 26 \pm 6$ MeV in the charged channel and $M = 1684 \pm 5$ MeV and $\Gamma = 20 \pm 4$ MeV in the neutral channel. In Ref. [13],

the $\Xi^*(1690)$ resonance was confirmed by the WA89 Collaboration in the neutral $\pi^+\Xi^-$ channel with measured mass $M = 1686 \pm 4$ MeV and width $\Gamma = 10 \pm 6$ MeV. In Ref. [14], in addition to the investigations of the $\Xi^*(1530)$ properties in the $\Lambda_c^+ \rightarrow K^+ \pi^+ \Xi^-$ decay process, evidence of the existence of the $\Xi^*(1690)$ resonance with $J^P = 1/2^-$ was also found by the BABAR Collaboration. In Ref. [15], the Belle Collaboration presented the first evidence for the process $\Lambda_c^+ \rightarrow K^+ \Xi^{*0}(1690) \rightarrow K^+ K^- \Sigma^+$, and the fitted mass and width of $\Xi^*(1690)$ are $M = 1688 \pm 2$ MeV and $\Gamma = 11 \pm 4$ MeV. Furthermore, the contribution of the $\Xi^{*0}(1690)$ to the $\Lambda_c^+ \rightarrow K^+ \Xi^{*0}(1690) \rightarrow K^+ \bar{K}^0 \Lambda$ reaction was also found [15]. In Ref. [16], the $\Xi(1690)$ resonance was also observed in the $\bar{K}^0 \Lambda$ channel in the decay $\Lambda_c^+ \rightarrow K^+ \bar{K}^0 \Lambda$ by the BABAR Collaboration, where a coherent amplitude analysis of the $\Lambda a_0(980)$ and $K^+ \Xi^{*0}(1690)$ productions was performed; the obtained mass and width of the $\Xi^*(1690)$ resonance are $M = 1684.7 \pm 1.3(\text{stat})_{-1.6}^{+2.2}(\text{syst})$ MeV, $\Gamma = 8.1_{-3.5}^{+3.9}(\text{stat})_{-0.9}^{+1.0}(\text{syst})$ MeV, and its spin is consistent with $1/2$. Furthermore, the $\Xi^*(1690)$ resonance has also been found in the hyperon-nucleon interactions [17,18]. In most of these experimental analyses, the spin parity of $\Xi^*(1690)$ resonance favor $J^P = 1/2^-$.

In 2019, the $\Xi^*(1620)$ resonance was observed in the $\pi^+\Xi^-$ invariant spectrum via the $\Xi_c^+ \rightarrow \Xi^- \pi^+ \pi^+$ decay. Meanwhile, the evidence of the $\Xi^*(1690)$ resonance was also found with the same data sample, and its significance

*liusiwei@impcas.ac.cn

†shenqinghua@impcas.ac.cn

‡xiejujun@impcas.ac.cn

Published by the American Physical Society under the terms of the [Creative Commons Attribution 4.0 International license](https://creativecommons.org/licenses/by/4.0/). Further distribution of this work must maintain attribution to the author(s) and the published article's title, journal citation, and DOI. Funded by SCOAP³.

is 4σ [19]. However, so far the quantum numbers of $\Xi^*(1690)$ have not yet been determined. Therefore, to fully understand the nature of the $\Xi^*(1690)$ resonance, further experiments are certainly required.

On the theoretical side, within the constituent quark models, the first excited state of the Ξ baryon is around 1800 MeV [20–22], and thus it is difficult to treat $\Xi^*(1690)$ as a three-quark state. In Ref. [3], the $\Xi^*(1690)$ was treated as a three-quark state and its spin-parity quantum numbers are $J^P = 1/2^-$. Note that the obtained mass with the constituent quark model [3] is 1725 MeV, which is still 35 MeV higher than its nominal mass. This implies that $\Xi^*(1690)$ might have some nontrivial structure other than the usual three-quark state. In fact, using the chiral unitary approach, the $\Xi^*(1690)$ can be interpreted as an s -wave meson-baryon molecular state [1,2,23]. It couples strongly to the $\bar{K}\Sigma$ channel [23], and its coupling to the $\pi\Xi$ channel is small. Thus, its narrow width can be naturally explained [23]. Furthermore, its spin parity is $1/2^-$ in the chiral unitary approach. In Ref. [24], the $\Xi^*(1690)$ was investigated by means of the two-point QCD sum rules, where it was also concluded that the $\Xi^*(1690)$ state most probably has spin-parity quantum numbers $J^P = 1/2^-$. However, the obtained width for the $\Xi^*(1690)$ state is about 100 MeV [24], which is much larger than the experimental measurements [6].

The main property of the $\Xi^*(1690)$ resonance is that its decay width is too narrow compared with other baryon resonances that have similar masses [6]. In spite of the fact that the $\Xi^*(1690)$ state has a large phase space to decay to open channels, such as $\pi\Xi$ and $\bar{K}\Lambda$, its width is just on the order of 10 MeV. In Ref. [25], using the chiral unitary approach, the $\Xi^*(1690)$ state was dynamically generated in the pseudoscalar-baryon and vector-baryon coupled channels.¹ It was found that most of the properties of $\Xi^*(1690)$, especially its narrow width, can be well explained [25]. In that work, the $\Xi^*(1690)$ had strong couplings to $\bar{K}\Sigma$ and $\eta\Xi$ channels, while its couplings to the $\bar{K}\Lambda$ and $\pi\Xi$ channels were small. Recently, the meson-baryon interaction in the neutral strangeness $S = -2$ sector was studied using an extended unitarized chiral perturbation theory, where the leading Weinberg-Tomozawa term, Born term, and the next-to-leading-order contributions were considered [26]. It was found that both the $\Xi^*(1620)$ and $\Xi^*(1690)$ states can be dynamically generated, and their obtained properties are in reasonable agreement with the known experimental data.

It has been shown that the weak decay of charmed baryons governed by the $c \rightarrow s$ quark transition is beneficial to probe the strange baryons, some of which are

¹Note that the transitions between pseudoscalar-baryon and vector-baryon channels are crucial to obtain the pole for the $\Xi^*(1690)$ state. If these transitions were zero, the pole of $\Xi^*(1690)$ would disappear.

subjects of intense debate about their nature [27–29]. For instance, the hyperon production from the $\Lambda_c^+ \rightarrow K^- p \pi^+$ and $\Lambda_c^+ \rightarrow K_S^0 p \pi^0$ decays were investigated within the effective Lagrangian approach in Ref. [30]. The $\Xi^*(1620)$ and $\Xi^*(1690)$ states were studied in the $\Xi_c \rightarrow \pi^+ M B$ process in Ref. [31], where M and B stand for mesons and baryons, respectively. It was shown that these weak decays might be an ideal tool to study the $\Xi^*(1620)$ and $\Xi^*(1690)$ resonances, which are dynamically produced in the rescattering of M and B in the final states.

Therefore, in this work we take advantage of these ideas and revisit the $\Lambda_c^+ \rightarrow \Lambda K^+ \bar{K}^0$ decay, which requires the creation of an $s\bar{s}$ quark pair. Following Refs. [23,25,31], in addition to the contributions of the $\Xi^*(1690)$ resonance that is dynamically generated from the final-state interactions of $\bar{K}^0\Lambda$ in the S wave, we also consider the contributions of the $a_0(980)$ and $N^*(1535)$ states, where they are dynamically produced by the final-state interactions of $K^+\bar{K}^0$ [32,33] and ΛK^+ [34–39] in coupled channels, respectively. One can see that the treatment of the $\Xi^*(1690)$ and $a_0(980)$ resonances is different than that used in Ref. [16], where the Breit-Wigner form of their propagators was used.

This article is organized as follows. In the next section, we present the theoretical formalism for studying the $\Lambda_c^+ \rightarrow \Lambda K^+ \bar{K}^0$ decay. In Sec. III, theoretical numerical results and discussions are presented, followed by a short summary in Sec. IV.

II. FORMALISM

For the production of $\Xi^*(1690)$ in the weak decay process $\Lambda_c^+ \rightarrow K^+ \bar{K}^0 \Lambda$, we first take it as a dynamically generated state in the final-state interaction of $\bar{K}\Lambda$ in coupled channels. Second, we take $\Xi^*(1690)$ as a Breit-Wigner resonance. The roles of $a_0(980)$ and $N^*(1535)$ are also investigated, where the contribution of the $a_0(980)$ state is encoded in the s -wave $K\bar{K}$ final-state interaction, as done in Refs. [40–45], and that of the $N^*(1535)$ resonance is in the s -wave $K\Lambda$ final-state interaction [34–39].

The schematic diagram for the Cabibbo-favored process $\Lambda_c^+ \rightarrow \Lambda K^+ \bar{K}^0$ is presented in Fig. 1, where the decay process proceeds in three parts:

- (1) In the first step, the c quark in Λ_c^+ turns into an s quark via the weak decay.

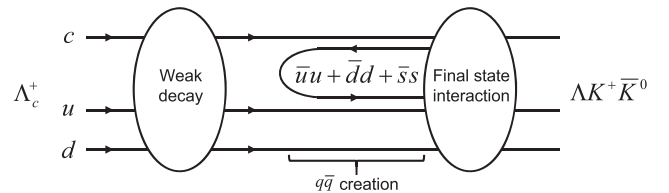
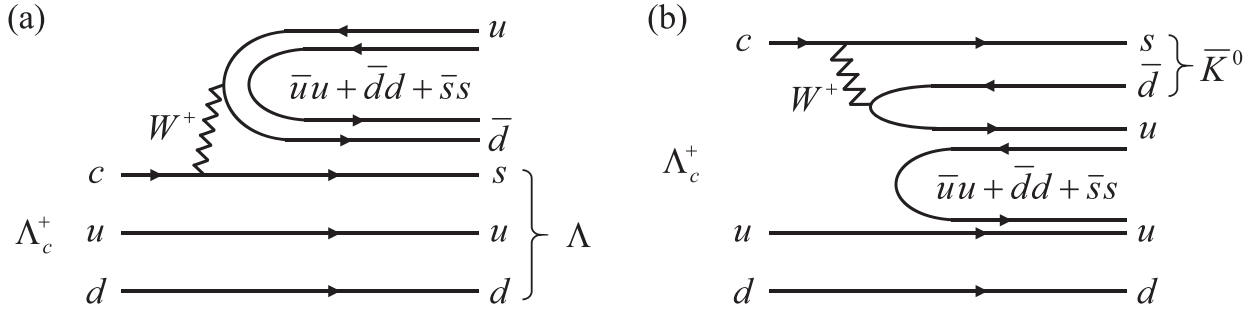


FIG. 1. Schematic diagram for the Cabibbo-favored process $\Lambda_c^+ \rightarrow \Lambda K^+ \bar{K}^0$.

FIG. 2. Decay mechanisms for (a) $\Lambda_c^+ \rightarrow \Lambda + (PP)^+$ and (b) $\Lambda_c^+ \rightarrow \bar{K}^0 + (PB)^+$.

- (2) A $q\bar{q}$ pair with the quantum numbers of the vacuum is introduced to form a pseudoscalar-baryon (PB) or pseudoscalar-pseudoscalar (PP) pair.
- (3) The final-state interactions are taken into account in coupled channels within the chiral unitary approach, which will lead to the dynamical productions of the $a_0(980)$, $N^*(1535)$, and $\Xi^*(1690)$ resonances.

A. Contributions of the $a_0(980)$, $N^*(1535)$, and $\Xi^*(1690)$ resonances from final-state interactions

Following Refs. [31,46–50], we assume two primary decay mechanisms for the process $\Lambda_c^+ \rightarrow \Lambda K^+ \bar{K}^0$, which are presented in Fig. 2. In the weak decay of charmed hadrons the diagrams are classified into six different topologies [51–54]: W external emission, W internal emission, W exchange, W annihilation, horizontal W loop, and vertical W loop. Here, we consider the dominant W external emission and internal emission diagrams as shown in Figs. 2(a) and 2(b), respectively. The c quark in Λ_c^+ turns into an s quark and a W^+ boson, followed by the W^+ boson decaying into a $u\bar{d}$ pair. To get the final states $\Lambda K^+ \bar{K}^0$, the sud ($s\bar{d}$) cluster forms the Λ (\bar{K}^0), and the $u\bar{d}$ (uud), together with the $q\bar{q}$ ($= u\bar{u} + d\bar{d} + s\bar{s}$) pair created from the vacuum, hadronize into $K^+ \bar{K}^0$ ($K^+ \Lambda$). In the former processes, the ud diquark in the Λ_c^+ is always kept. Therefore, the Λ_c^+ weak decay processes shown in Fig. 2 can be formulated as follows [46–50]:

$$\begin{aligned} \Lambda_c^+ &= \frac{1}{\sqrt{2}} |c(ud - du)\rangle \\ &\rightarrow -\frac{\sqrt{6}}{3} V_1 |\Lambda\rangle |u(u\bar{u} + d\bar{d} + s\bar{s})\bar{d}\rangle \end{aligned} \quad (1)$$

$$\rightarrow \frac{1}{\sqrt{2}} V_2 |\bar{K}^0\rangle |u(u\bar{u} + d\bar{d} + s\bar{s})(ud - du)\rangle, \quad (2)$$

where V_1 and V_2 are the strength of the production vertices,² which contain all of the dynamical factors.

²We assume that these production vertices proceed through S -wave interaction.

According to these results of Ref. [31], we then connect two degrees of freedom: the quarks and the hadrons. Then, we can rewrite the intermediate states as

$$\Lambda_c^+ \rightarrow V_1 |\Lambda\rangle \left| -\frac{2\sqrt{2}}{3} \pi^+ \eta - \frac{\sqrt{6}}{3} K^+ \bar{K}^0 \right\rangle \quad (3)$$

$$\rightarrow V_2 |\bar{K}^0\rangle \left| \left(\frac{\eta}{\sqrt{3}} + \frac{\pi^0}{\sqrt{2}} \right) p + \pi^+ n - \frac{\sqrt{6}}{3} K^+ \Lambda \right\rangle, \quad (4)$$

where we have omitted the η' terms as in Refs. [23,25,31] because its mass threshold is located much high and its contribution should be small. After the production of the PP or PB pair, the final-state interactions between intermediate mesons and baryons arise, as shown in Fig. 3. We can also obtain the explicit expressions of the decay amplitude \mathcal{M}_i ($i = a, b, c$, and d according to the diagrams shown in Fig. 3) using Eqs. (3) and (4):

$$\mathcal{M}_a = \mathcal{M}^{\text{Tree}} = -\frac{\sqrt{6}}{3} (V_1 + V_2), \quad (5)$$

$$\begin{aligned} \mathcal{M}_b &= \mathcal{M}_{K^+ \bar{K}^0}^{\text{FSI}} \\ &= h_{K^+ \bar{K}^0} G_{K^+ \bar{K}^0} T_{K\bar{K} \rightarrow K\bar{K}}^{I=1} - h_{\pi^+ \eta} G_{\pi^+ \eta} T_{\pi\eta \rightarrow K\bar{K}}^{I=1}, \end{aligned} \quad (6)$$

$$\mathcal{M}_c = \mathcal{M}_{\bar{K}^0 \Lambda}^{\text{FSI}} = h_{\bar{K}^0 \Lambda} G_{\bar{K}^0 \Lambda} T_{\bar{K}\Lambda \rightarrow \bar{K}\Lambda}^{I=1/2}, \quad (7)$$

$$\begin{aligned} \mathcal{M}_d &= \mathcal{M}_{K^+ \Lambda}^{\text{FSI}} \\ &= h_{K^+ \Lambda} G_{K^+ \Lambda} T_{K\Lambda \rightarrow K\Lambda}^{I=1/2} \\ &\quad - \left(\sqrt{\frac{2}{3}} h_{\pi^+ n} G_{\pi^+ n} + \frac{1}{\sqrt{3}} h_{\pi^0 p} G_{\pi^0 p} \right) T_{\pi N \rightarrow K\Lambda}^{I=1/2} \\ &\quad + h_{\eta p} G_{\eta p} T_{\eta N \rightarrow K\Lambda}^{I=1/2}, \end{aligned} \quad (8)$$

where G_{PP} and G_{PB} are the loop functions of the PP or PB propagator, respectively. The coefficients h_{PP} and h_{PB} for the terms of final-state interactions are

$$h_{K^+ \bar{K}^0} = -\frac{\sqrt{6}}{3} (V_1 + V_2), \quad h_{\pi^+ \eta} = -\frac{2\sqrt{2}}{3} V_1, \quad (9)$$

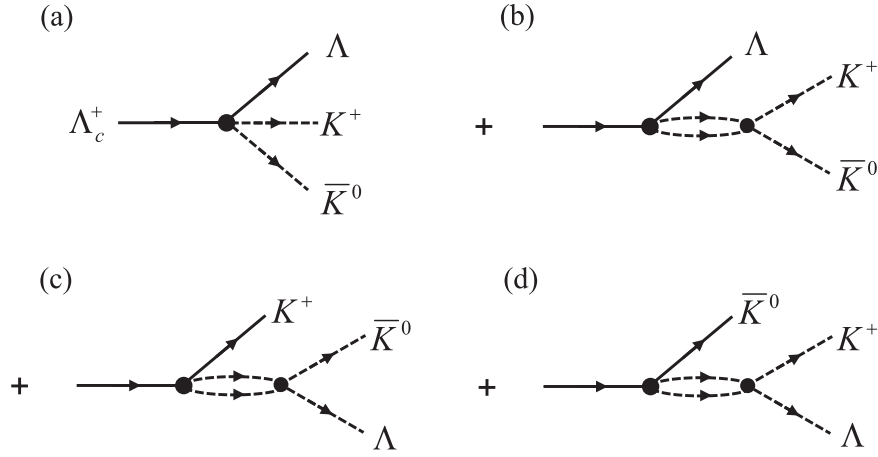


FIG. 3. Schematic diagram for the final-state interaction for the $\Lambda_c^+ \rightarrow \Lambda K^+ \bar{K}^0$ decay. (a) tree-level diagram. (b) $K^+ \bar{K}^0$ rescattering. (c) $\bar{K}^0 \Lambda$ rescattering. (d) $K^+ \Lambda$ rescattering.

$$h_{\bar{K}^0 \Lambda} = h_{K^+ \Lambda} = -\frac{\sqrt{6}}{3}(V_1 + V_2), \quad (10)$$

$$h_{\pi^+ n} = V_2, \quad h_{\pi^0 p} = \frac{\sqrt{2}}{2}V_2, \quad h_{\eta p} = \frac{\sqrt{3}}{3}V_2. \quad (11)$$

The analytic form of the loop function G , with dimensional regularization, is given by

$$G(s) = \frac{2M}{16\pi^2} \left\{ a_\mu + \ln \frac{M^2}{\mu^2} + \frac{m^2 - M^2 + s}{2s} \ln \frac{m^2}{M^2} \right. \\ \left. + \frac{p}{\sqrt{s}} [\ln(s - (m^2 - M^2) + 2p\sqrt{s}) \right. \\ \left. + \ln(s + (m^2 - M^2) + 2p\sqrt{s}) \right. \\ \left. - \ln(-s + (m^2 - M^2) + 2p\sqrt{s}) \right. \\ \left. - \ln(-s - (m^2 - M^2) + 2p\sqrt{s}) \right\}, \quad (12)$$

where μ is a scale of dimensional regularization and a_μ is the subtraction constant. Any change of μ can be reabsorbed by a change in a_μ . In this work, we choose $\mu = 630$ MeV while a_μ will be determined from the experimental data, both of which we discuss in the following. m and M are the masses of the meson and baryon in the loop, respectively. p represents the magnitude of the three-momentum of one particle in the meson-meson or meson-baryon rest frame,

$$p = \frac{\lambda^{1/2}(s, m^2, M^2)}{2\sqrt{s}}, \quad (13)$$

$$\lambda^{1/2}(x, y, z) = \sqrt{x^2 + y^2 + z^2 - 2xy - 2yz - 2xz}. \quad (14)$$

The two-body scattering amplitudes $T_{PP \rightarrow PP}$ and $T_{PB \rightarrow PB}$ are obtained by solving the Bethe-Salpeter equation within the chiral unitary approach [33,55,56],

$$T = [1 - VG]^{-1}V, \quad (15)$$

where V is the transition potential between the involved channels, which were given explicitly in Refs. [25,33,39,57]. The scattering amplitude element T in Eq. (15) in the particle basis can be related to the one in the isospin basis, and we get

$$T_{K^+ \bar{K}^0 \rightarrow K^+ \bar{K}^0} = T_{K\bar{K} \rightarrow K\bar{K}}^{I=1}, \quad (16)$$

$$T_{\pi^+ \eta \rightarrow K^+ \bar{K}^0} = -T_{\pi\eta \rightarrow K\bar{K}}^{I=1}, \quad (17)$$

$$T_{\bar{K}^0 \Lambda \rightarrow \bar{K}^0 \Lambda} = T_{\bar{K}\Lambda \rightarrow \bar{K}\Lambda}^{I=1/2}, \quad (18)$$

$$T_{K^+ \Lambda \rightarrow K^+ \Lambda} = T_{K\Lambda \rightarrow K\Lambda}^{I=1/2}, \quad (19)$$

$$T_{\pi^+ n \rightarrow K^+ \Lambda} = -\sqrt{\frac{2}{3}} T_{\pi N \rightarrow K\Lambda}^{I=1/2}, \quad (20)$$

$$T_{\pi^0 p \rightarrow K^+ \Lambda} = -\sqrt{\frac{1}{3}} T_{\pi N \rightarrow K\Lambda}^{I=1/2}, \quad (21)$$

$$T_{\eta p \rightarrow K^+ \Lambda} = T_{\eta N \rightarrow K\Lambda}^{I=1/2}. \quad (22)$$

Although the forms of these $K\bar{K}$, $K\Lambda$, and $\bar{K}\Lambda$ interactions have been detailed elsewhere [25,33,36,39,57,58], here we briefly revisit the $\bar{K}\Lambda$ case. This will allow us to review the general procedure of calculating the two-body amplitudes entering the total decay amplitude of the $\Lambda_c^+ \rightarrow \Lambda \bar{K}^0 K^+$ reaction.

In order to describe the $\Xi^*(1690)$ state we perform a coupled channel analysis. In the isospin-1/2 sector, there are four coupled channels: $\pi\Xi$, $\bar{K}\Lambda$, $\bar{K}\Sigma$, and $\eta\Xi$.

TABLE I. Coefficients C_{ij} for $\pi\Xi$, $\bar{K}\Lambda$, $\bar{K}\Sigma$, and $\eta\Xi$ coupled channels in the isospin $I = 1/2$ basis.

	$\pi\Xi$	$\bar{K}\Lambda$	$\bar{K}\Sigma$	$\eta\Xi$
$\pi\Xi$	2	-3/2	-1/2	0
$\bar{K}\Lambda$		0	0	-3/2
$\bar{K}\Sigma$			2	3/2
$\eta\Xi$				0

These channels are labeled by the indices $j = 1, \dots, 4$. The transition potential V_{ij} is expressed as [25,58]

$$V_{ij} = -\frac{C_{ij}}{4f_i f_j} (2\sqrt{s} - M_i - M_j) \times \sqrt{\frac{(M_i + E_i)(M_j + E_j)}{4M_i M_j}}, \quad (23)$$

where f_i is the meson decay constant of the i th channel, $f_\pi = 92.1$ MeV, $f_K = 1.2f_\pi$, and $f_\eta = 1.3f_\pi$. E_i and E_j are the initial and final baryon energies respectively, and $E_i = \sqrt{M_i^2 + |\vec{p}_i|^2}$, $|\vec{p}_i| = \frac{\lambda^{1/2}(s, m_i^2, M_i^2)}{2\sqrt{s}} \theta(\sqrt{s} - M_i - m_i)$, where s is the invariant mass squared of the meson-baryon system and m_i and M_i are the meson and baryon masses in the i th channel, respectively. The factor C_{ij} is symmetric and its value is listed in Table I.

Then, one can solve the Bethe-Salpeter equation as shown in Eq. (15) with the on-shell factorized potential and, thus, the S -wave scattering T_{ij} matrix can be easily obtained. Then, one can also look for poles of the scattering amplitude T_{ij} on the complex plane of \sqrt{s} . The pole Z_R on the second Riemann sheet could be associated with the $\Xi^*(1690)$ resonance. The real part of Z_R is associated with the mass $M_{\Xi^*(1690)}$ of the $\Xi^*(1690)$ resonance, and the imaginary part of Z_R is associated with one half of its width $\Gamma_{\Xi^*(1690)}$.

B. Contribution of the $\Xi^*(1690)$ resonance as a Breit-Wigner resonance

On the other hand, the decay process $\Lambda_c^+ \rightarrow \Xi^*(1690)K^+ \rightarrow \Lambda \bar{K}^0 K^+$ can also proceed through $\Xi^*(1690)$ as a Breit-Wigner resonance and decay into $\bar{K}^0\Lambda$, which is shown in Fig. 4. In this case, the $\Xi^*(1690)$ state is formed with $u\bar{d}s\bar{s}$, as shown in Fig. 4(a), and it decays into $\bar{K}^0\Lambda$ in the final state. The hadron-level diagram for the decay of $\Lambda_c^+ \rightarrow \Xi^*(1690)K^+ \rightarrow \Lambda K^+ \bar{K}^0$ is also shown in Fig. 4(b), where the propagator of the $\Xi^*(1690)$ resonance is parametrized as the Breit-Wigner form.

Then, the general decay amplitude for the process $\Lambda_c^+ \rightarrow \Xi^*(1690)^0 K^+ \rightarrow \bar{K}^0 \Lambda K^+$ can be expressed as

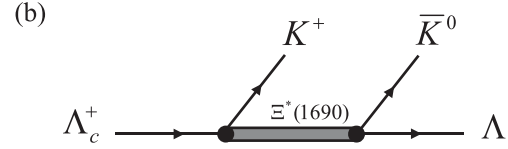
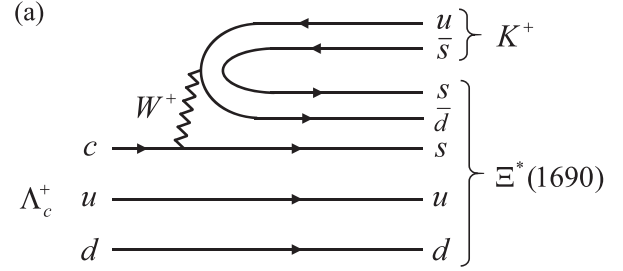


FIG. 4. (a) Quark-level diagram for the $\Lambda_c^+ \rightarrow K^+ \Xi^*(1690)$ decay and (b) hadron-level diagram for the $\Lambda_c^+ \rightarrow K^+ \Xi^*(1690) \rightarrow K^+ \bar{K}^0 \Lambda$ decay.

$$\mathcal{M}_e = \frac{\Gamma_{\Xi^*(1690)}}{2} \frac{V_3}{M_{\bar{K}^0\Lambda} - M_{\Xi^*(1690)} + i \frac{\Gamma_{\Xi^*(1690)}}{2}}, \quad (24)$$

where $M_{\bar{K}^0\Lambda}$ is the invariant mass of the $\bar{K}^0\Lambda$ system and we take $M_{\Xi^*(1690)} = 1690$ MeV and $\Gamma_{\Xi^*(1690)} = 20$ MeV for the Breit-Wigner mass and width for the $\Xi^*(1690)$ resonance, respectively, which are quoted in the PDG [6]. The model free parameter V_3 will be determined by the experimental data.

Before going further, we emphasize that the $u\bar{d}s\bar{s}$ component of the $\Xi^*(1690)$ resonance cannot be guaranteed from the decay process shown in Fig. 4. Indeed, the $\Xi^*(1690)$ resonance can also be produced from the W -exchange diagram [15,59–61], where cd transitions first into su with the weak interaction, and then with a $s\bar{s}$ pair from the vacuum, the $u\bar{s}$ forms the K^+ , while the $\Xi^*(1690)^0$ is constructed from the uss cluster and then it decays into $\bar{K}^0\Lambda$. Nevertheless, this kind of contributions can be absorbed into the model parameter V_3 .

C. Invariant mass distributions of the $\Lambda_c^+ \rightarrow \Lambda K^+ \bar{K}^0$ decay

With the ingredients obtained in the previous sections, we can write the double invariant mass distributions for the $\Lambda_c^+ \rightarrow K^+ \bar{K}^0 \Lambda$ decay as

$$\frac{d^2\Gamma}{dM_{K^+\bar{K}^0} dM_{\bar{K}^0\Lambda}} = \frac{M_\Lambda M_{K^+\bar{K}^0} M_{\bar{K}^0\Lambda}}{16\pi^3 M_{\Lambda_c^+}^2} |\mathcal{M}|^2, \quad (25)$$

where \mathcal{M} is the total decay amplitude. We take two models for \mathcal{M} :

$$\mathcal{M}^I = \mathcal{M}_a + \mathcal{M}_b + \mathcal{M}_d + \mathcal{M}_c, \quad (26)$$

$$\mathcal{M}^{\Pi} = \mathcal{M}_a + \mathcal{M}_b + \mathcal{M}_d + e^{i\theta} \mathcal{M}_e, \quad (27)$$

where a relative phase θ is added for Model II, and it is a free parameter. In addition, another relative phase, ϕ , between V_1 and V_2 is also taken into account. We replace V_2 with $e^{i\phi}V_2$ in the following fitting process. Furthermore, it is worth mentioning that V_1 , V_2 , and V_3 have dimension MeV^{-1} .

Then, the invariant $\bar{K}^0\Lambda$ and $K^+\bar{K}^0$ mass distributions can be obtained by integrating over the other invariant mass in Eq. (25). For a given value of $M_{\bar{K}^0\Lambda}$, the invariant mass $M_{K^+\bar{K}^0}$ satisfies the following relation:

$$\begin{aligned} (M_{K^+\bar{K}^0}^{\min})^2 &= (E_{K^+} + E_{\bar{K}^0})^2 \\ &\quad - \left(\sqrt{E_{K^+}^2 - m_{K^+}^2} + \sqrt{E_{\bar{K}^0}^2 - m_{\bar{K}^0}^2} \right)^2, \\ (M_{K^+\bar{K}^0}^{\max})^2 &= (E_{K^+} + E_{\bar{K}^0})^2 \\ &\quad - \left(\sqrt{E_{K^+}^2 - m_{K^+}^2} - \sqrt{E_{\bar{K}^0}^2 - m_{\bar{K}^0}^2} \right)^2, \end{aligned} \quad (28)$$

where E_{K^+} and $E_{\bar{K}^0}$ are the particle energies in the $\bar{K}^0\Lambda$ rest frame, which can be expressed explicitly as

$$\begin{aligned} E_{K^+} &= \frac{M_{\Lambda_c^+}^2 - M_{\bar{K}^0\Lambda}^2 - M_{K^+}^2}{2M_{\bar{K}^0\Lambda}}, \\ E_{\bar{K}^0} &= \frac{M_{\bar{K}^0\Lambda}^2 + M_{K^+}^2 - M_{\Lambda_c^+}^2}{2M_{\bar{K}^0\Lambda}}. \end{aligned} \quad (29)$$

Note that the invariant $K^+\Lambda$ mass distribution can be obtained by substituting $M_{K^+\bar{K}^0}$ with $M_{K^+\Lambda}$.

III. RESULTS AND DISCUSSION

With the above formalism, we perform the χ^2 fits to the experimental data on the invariant mass distributions of the process $\Lambda_c^+ \rightarrow \Lambda K^+ \bar{K}^0$. There are a total of 79 data points. For Model I, there are five free parameters: V_1 , V_2 , $a_{\bar{K}\Sigma}$, $a_{\eta\Xi}$, and ϕ . For Model II, there are also five free parameters: V_1 , V_2 , V_3 , ϕ , and θ . Note that we have fixed $a_{\pi\Xi} = a_{\bar{K}\Lambda} = -2$ as their natural value, and $a_{\bar{K}\Sigma}$ and $a_{\eta\Xi}$ are free parameters in this work. It is found that the pole position of the $\Xi^*(1690)$ state is not sensitive to the values of $a_{\pi\Xi}$ and $a_{\bar{K}\Lambda}$, as found in Refs. [23,58].

The fitted parameters and the corresponding $\chi^2/\text{d.o.f.}$ are listed in Table II. One can find that both fits in Table II show reasonably small $\chi^2/\text{d.o.f.}$ With the fitted parameters $a_{\bar{K}\Sigma}$ and $a_{\eta\Xi}$, the pole position of the $\Xi^*(1690)$ state is $M_R = 1685.83 + i2.76$ MeV, and the corresponding mass and width are $M_{\Xi^*(1690)} = 1685.83$ MeV, and $\Gamma_{\Xi^*(1690)} = 5.52$ MeV. The obtained mass of the $\Xi^*(1690)$ state is slightly below the mass threshold (1689 MeV) of the $\bar{K}\Sigma$ channel, and close to the averaged value quoted in the PDG. However, the obtained width is rather narrow,

TABLE II. Values of some of the parameters used or determined in this work. The values of $a_{\pi\Xi}$ and $a_{\bar{K}\Lambda}$ in Model I are fixed as the natural value -2 . The values of the mass and width for the $\Xi^*(1690)$ state are obtained from the fitted parameters of Model I. The mass and width of the $\Xi^*(1690)$ resonance for Model II are taken as $M_{\Xi^*} = 1690$ MeV and $\Gamma_{\Xi^*} = 20$ MeV, as quoted in the PDG [6].

	Model I	Model II
V_1 (MeV^{-1})	3.60 ± 0.55	0.45 ± 0.83
V_2 (MeV^{-1})	-0.89 ± 0.67	-4.61 ± 1.16
V_3 (MeV^{-1})	...	1.81 ± 0.18
$a_{\bar{K}\Sigma}$	-1.99 ± 0.09	...
$a_{\eta\Xi}$	-3.53 ± 0.29	...
ϕ	0.60 ± 0.45	3.20 ± 1.16
θ	...	0.67 ± 1.02
χ^2/dof	1.51	1.56
$M_{\Xi^*(1690)}$ (MeV)	1685.83 (output)	1690 (input)
$\Gamma_{\Xi^*(1690)}$ (MeV)	5.52 (output)	20 (input)

which is a common conclusion of the chiral unitary approach [23,25].

The fitted invariant mass distributions³ of the $\Lambda_c^+ \rightarrow \Lambda K^+ \bar{K}^0$ reaction are shown in Fig. 5 for Models I and II. It is found that both Models I and II can describe these experimental measurements fairly well. In Fig. 5(a), the peak of the $\Xi^*(1690)$ resonance in the ΛK_S^0 invariant mass distributions is well reproduced,⁴ and it is clearly seen that the line shapes of the $\Xi^*(1690)$ resonance are quite different for Models I and II. The peak produced from Model I is higher but narrower, and there is a sharp decrease around the mass threshold of the $\bar{K}\Sigma$ channel. As studied in Ref. [62], this sharp-decrease behavior is common in the coupled channel amplitudes if a higher and strong coupled channel was opened. For Model I, it is the $\bar{K}\Sigma$ channel [58], and around the mass threshold region of the $\bar{K}\Sigma$ channel there must be a dramatic change. In fact, this kind of behavior can also be described by the so-called Flatté parametrization for the Breit-Wigner distribution [63–65]. However, one needs a very strong coupling of the $\Xi^*(1690)$ resonance to the $\bar{K}\Sigma$ channel, which is unknown in Model II. Hence, we hope that more precise data, around the energy of $M_{\bar{K}^0\Lambda} = 1.69$ GeV, could be used to clarify this issue. Furthermore, one can see that without the

³To compare with the experimental measurements, we take $|K^0\rangle = \frac{1}{\sqrt{2}}(|K_S^0\rangle + |K_L^0\rangle)$ and $|\bar{K}^0\rangle = \frac{1}{\sqrt{2}}(|K_S^0\rangle - |K_L^0\rangle)$, where we have ignored the small effect of CP violation.

⁴It is worth pointing out that we have added an extra factor of $5/8$ to the theoretical results for the $\bar{K}^0\Lambda$ invariant mass distributions, since the experimental events were accumulated for a bin width of 5 MeV, while the events for the invariant $K^+K_S^0$ and $K^+\Lambda$ mass distributions are obtained in a bin width of 8 MeV.

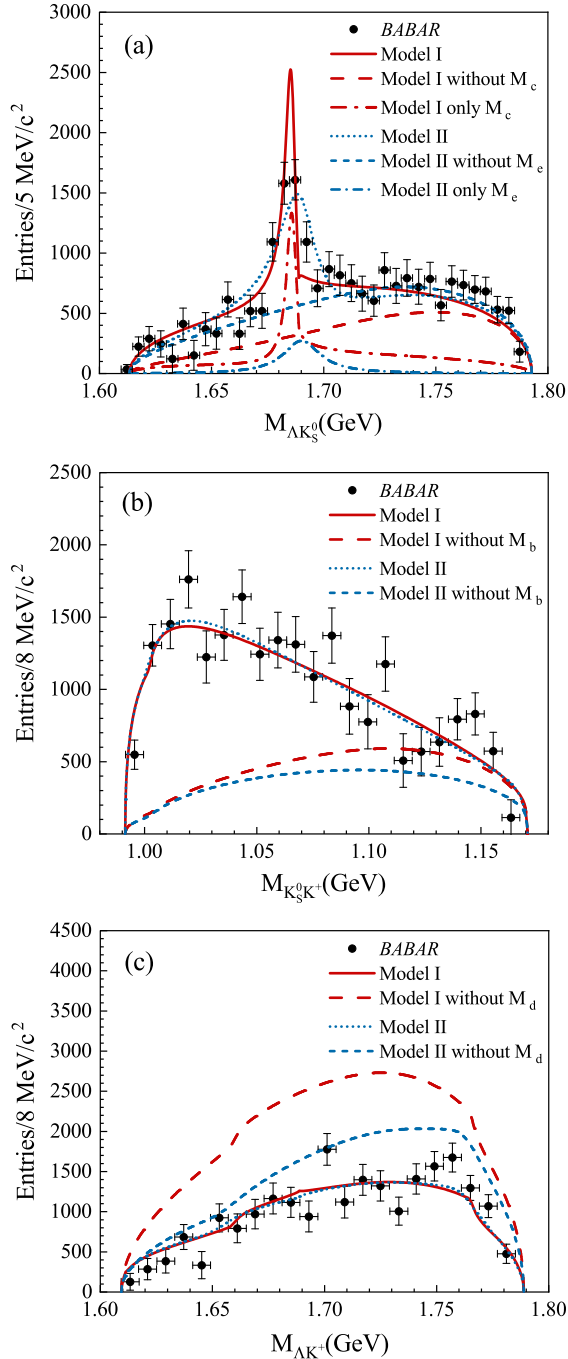


FIG. 5. Invariant mass distributions for the $\Lambda_c^+ \rightarrow \Lambda K^+ K_S^0$ reaction: (a) ΛK_S^0 invariant mass distributions, (b) the $K^+ K_S^0$ invariant mass distribution, and (c) the ΛK^+ invariant mass distribution.

contributions of $\Xi^*(1690)$ (\mathcal{M}_c for Model I, \mathcal{M}_e for Model II), the experimental data cannot be described.

On the other hand, near the $\bar{K}^0 \Lambda$ mass threshold, there is no enhancement that could be from the $\Xi^*(1620)$ resonance, which also couples strongly to the $\bar{K}^0 \Lambda$ channel. This might be because of the suppression of the small phase

space. Yet, further experimental data around the threshold are needed to clarify this issue.

For Model II, if the mass and width of the $\Xi^*(1690)$ resonance are not fixed, we can also get a good ($\chi^2/\text{d.o.f.} = 1.45$) and very similar fit as before. Moreover, the fitted line shape of $\Xi^*(1690)$ in this case is still very different than that of Model I. The fitted results for the mass and width of the $\Xi^*(1690)$ resonance are

$$M_{\Xi^*(1690)} = 1684.99 \pm 1.34 \text{ MeV}, \quad (30)$$

$$\Gamma_{\Xi^*(1690)} = 12.81 \pm 2.53 \text{ MeV}, \quad (31)$$

which are consistent with the results obtained by the Belle Collaboration [15] and BABAR Collaboration [16].

In Figs. 5(b) and 5(c) we show the $K_S^0 K^+$ and ΛK^+ invariant mass distributions, respectively. It is found that the theoretical results of Models I and II are very similar. This may indicate that the contributions of the $\Xi^*(1690)$ resonance, from Models I and II, to the $K_S^0 K^+$ and ΛK^+ invariant mass distributions are also similar, though they give very different line shapes for the $\Xi^*(1690)$ state. Once again, one can see that the contributions from the $K\bar{K}$ or $K\Lambda$ final-state interactions in the S -wave channel, as shown in Fig. 3, are crucial to reproduce the experimental measurements.

From Fig. 5(c), one can see that the interference cancellation between the \mathcal{M}_d term from the contributions of the $N^*(1535)$ resonance and the other terms is significant, especially for Model I. This may indicate that, regarding the current experimental data, the contributions of the $N^*(1535)$ resonance are unnecessary.⁵ Indeed, from the invariant ΛK^+ mass distributions, one cannot find evidence of the $N^*(1535)$ resonance near threshold. However, as shown in Fig. 3, after the production of $K^+ \Lambda$, their final-state interactions should be there. Hence, further studies on the final-state interactions of πN , ηN , $K\Lambda$, and $K\Sigma$ in coupled channels are needed, which is not the main purpose of this work.

Next, we study the Dalitz plot for the invariant masses of $K_S^0 \Lambda$ and $K^+ K_S^0$. The numerical results for Models I and II are shown in Figs. 6(a) and 6(b), respectively. From these figures, one can clearly see the signals for the $\Xi^*(1690)$ resonance in $K_S^0 \Lambda$, and the $a_0(980)$ resonance in $K^+ K_S^0$ close to its threshold. However, the signal for the $N^*(1535)$ resonance cannot be seen clearly, which might be because the mass of $N^*(1535)$ is far from the mass threshold of $K^+ \Lambda$. However, as discussed previously, the interference between $\Xi^*(1690)$ and $N^*(1535)$ in Model I is more destructive compared to that in Model II. Consequently, as the $M_{K^+ K_S^0}$ increases, the signal of the $\Xi^*(1690)$

⁵We have checked that the contributions of the $N^*(1535)$ resonance to the $K_S^0 \Lambda$ and $K^+ K_S^0$ invariant mass distributions are tiny.

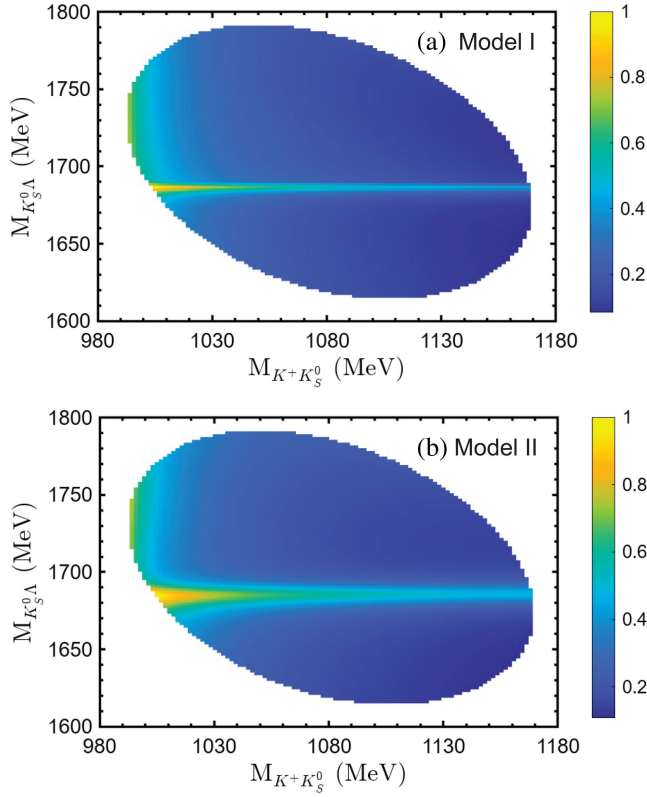


FIG. 6. Dalitz plot representation for the invariant masses of $K_S^0\Lambda$ and $K^+K_S^0$.

resonance in Model I decreases much more rapidly than in Model II, with the contribution of the $N^*(1535)$ resonance being a factor in this behavior.

Finally, we study the branching fractions of the $\Lambda_c^+ \rightarrow K^+\Xi^*(1690) \rightarrow K^+\bar{K}^0\Lambda$ decay to see the effect of the $\Xi^*(1690)$ resonance in the process $\Lambda_c^+ \rightarrow \Lambda K^+\bar{K}^0$. With the full amplitude of Eqs. (26) and (27) and the fitted parameters shown in Table II, the numerical result for the branching fraction of the production of the $\Xi^*(1690)$ resonance can be calculated as

$$\frac{\mathcal{B}(\Lambda_c^+ \rightarrow K^+\Xi^*(1690) \rightarrow K^+\bar{K}^0\Lambda)}{\mathcal{B}(\Lambda_c^+ \rightarrow \Lambda K^+\bar{K}^0)} = \begin{cases} 0.28, \\ 0.07 \end{cases} \quad (32)$$

for Models I and II, respectively. The above result for Model I is in good agreement with the experimental data of the Belle Collaboration, $0.26 \pm 0.08 \pm 0.03$ [15], while the result for Model II is much smaller. This can be easily

understood from the numerical results shown in Fig. 5(a). For Model I, although the line shape of the $\Xi^*(1690)$ resonance is narrower, it is much higher than the results obtained from Model II. In addition, if the fitted parameters that the mass and width of $\Xi^*(1690)$ are free in Model II, the above ratio in Eq. (32) is 0.06. We hope that the calculations here can be checked by future precise experiments, which will be useful to understand the nature of the $\Xi^*(1690)$ resonance.

IV. SUMMARY

In this work, we have performed an analysis of the $\Lambda_c^+ \rightarrow \Lambda K^+\bar{K}^0$ decay via two Cabibbo-favored mechanisms. By considering the hadronization process and the final-state interaction in the pseudoscalar-baryon and pseudoscalar-pseudoscalar channels with the chiral unitary approach, the role of the $\Xi^*(1690)$, $a_0(980)$, and $N^*(1535)$ resonances were investigated. Taking into account the contributions of these three resonances, we calculated the $K^+K_S^0$, ΛK_S^0 and ΛK^+ invariant mass distributions. Up to five free parameters, we performed a χ^2 fit to the experimental measurements. We found that the reaction proposed here can describe the experimental data of the BABAR Collaboration [16]. In particular, the clear signal for the $\Xi^*(1690)$ state can be well reproduced in the ΛK_S^0 invariant mass spectrum.

Within the fitted model parameters, we further calculated the ratio of the branching fractions $\mathcal{B}(\Lambda_c^+ \rightarrow K^+\Xi^*(1690) \rightarrow K^+\bar{K}^0\Lambda)/\mathcal{B}(\Lambda_c^+ \rightarrow \Lambda K^+\bar{K}^0)$ to see the contribution of the $\Xi^*(1690)$ resonance in the $\Lambda_c^+ \rightarrow \Lambda K^+\bar{K}^0$ decay. The obtained value 0.28 for Model I, where the $\Xi^*(1690)$ is dynamically generated from the meson-baryon final-state interactions, is consistent with the experimental value from the Belle Collaboration [15]. It is expected that the $\Xi^*(1690)$ state can be analyzed from the precise measurements of the $\Lambda_c^+ \rightarrow K^+\bar{K}^0\Lambda$ decay by the BESIII, BelleII, and LHCb collaborations in the future [66].

ACKNOWLEDGMENTS

We would like to thank Wei-Hong Liang and Eulogio Oset for useful discussions. This work is partly supported by the National Natural Science Foundation of China under Grant No. 12075288. It is also supported by the Youth Innovation Promotion Association CAS.

- [1] C. Garcia-Recio, M. F. M. Lutz, and J. Nieves, *Phys. Lett. B* **582**, 49 (2004).
- [2] D. Gamermann, C. Garcia-Recio, J. Nieves, and L. L. Salcedo, *Phys. Rev. D* **84**, 056017 (2011).
- [3] M. Pervin and W. Roberts, *Phys. Rev. C* **77**, 025202 (2008).
- [4] M. Pavon Valderrama, J.-J. Xie, and J. Nieves, *Phys. Rev. D* **85**, 017502 (2012).
- [5] T. Nishibuchi and T. Hyodo, *EPJ Web Conf.* **271**, 10002 (2022).
- [6] P. A. Zyla *et al.* (Particle Data Group), *Prog. Theor. Exp. Phys.* **2020**, 083C01 (2020).
- [7] T. Nagae, *AIP Conf. Proc.* **773**, 6 (2005).
- [8] L. Guo *et al.*, *Phys. Rev. C* **76**, 025208 (2007).
- [9] R. Schumacher (CLAS Collaboration), *AIP Conf. Proc.* **1257**, 100 (2010).
- [10] M. F. M. Lutz *et al.* (PANDA Collaboration), *arXiv:0903.3905*.
- [11] J. K. Ahn and S.-i. Nam, *Phys. Rev. D* **98**, 114012 (2018).
- [12] C. Dionisi *et al.* (Amsterdam-CERN-Nijmegen-Oxford Collaboration), *Phys. Lett. B* **80**, 145 (1978).
- [13] M. I. Adamovich *et al.* (WA99 Collaboration), *Eur. Phys. J. C* **5**, 621 (1998).
- [14] B. Aubert *et al.* (BABAR Collaboration), *Phys. Rev. D* **78**, 034008 (2008).
- [15] K. Abe *et al.* (Belle Collaboration), *Phys. Lett. B* **524**, 33 (2002).
- [16] B. Aubert *et al.* (BABAR Collaboration), in *Proceedings of the 33rd International Conference on High Energy Physics (2006)*, *arXiv:hep-ex/0607043*.
- [17] S. F. Biagi *et al.*, *Z. Phys. C* **9**, 305 (1981).
- [18] S. F. Biagi *et al.*, *Z. Phys. C* **34**, 15 (1987).
- [19] M. Sumihama *et al.* (Belle Collaboration), *Phys. Rev. Lett.* **122**, 072501 (2019).
- [20] K.-T. Chao, N. Isgur, and G. Karl, *Phys. Rev. D* **23**, 155 (1981).
- [21] S. Capstick and N. Isgur, *Phys. Rev. D* **34**, 2809 (1986).
- [22] L.-Y. Xiao and X.-H. Zhong, *Phys. Rev. D* **87**, 094002 (2013).
- [23] T. Sekihara, *Prog. Theor. Exp. Phys.* **2015**, 091D01 (2015).
- [24] T. M. Aliev, K. Azizi, and H. Sundu, *Eur. Phys. J. C* **78**, 396 (2018).
- [25] K. P. Khemchandani, A. Martínez Torres, A. Hosaka, H. Nagahiro, F. S. Navarra, and M. Nielsen, *Phys. Rev. D* **97**, 034005 (2018).
- [26] A. Feijoo, V. Valcarce Cadenas, and V. K. Magas, *Phys. Lett. B* **841**, 137927 (2023).
- [27] E. Oset *et al.*, *Int. J. Mod. Phys. E* **25**, 1630001 (2016).
- [28] E. Oset *et al.*, *Nucl. Phys.* **A954**, 371 (2016).
- [29] Y. Yu and Y.-K. Hsiao, *Phys. Lett. B* **820**, 136586 (2021).
- [30] J. K. Ahn, S. Yang, and S.-I. Nam, *Phys. Rev. D* **100**, 034027 (2019).
- [31] K. Miyahara, T. Hyodo, M. Oka, J. Nieves, and E. Oset, *Phys. Rev. C* **95**, 035212 (2017).
- [32] J. Nieves and E. Ruiz Arriola, *Phys. Lett. B* **455**, 30 (1999).
- [33] J. A. Oller and E. Oset, *Nucl. Phys.* **A620**, 438 (1997); **A652**, 407(E) (1999).
- [34] N. Kaiser, P. B. Siegel, and W. Weise, *Phys. Lett. B* **362**, 23 (1995).
- [35] J. Nieves and E. Ruiz Arriola, *Phys. Rev. D* **64**, 116008 (2001).
- [36] T. Inoue, E. Oset, and M. J. Vicente Vacas, *Phys. Rev. C* **65**, 035204 (2002).
- [37] P. C. Bruns, M. Mai, and U. G. Meissner, *Phys. Lett. B* **697**, 254 (2011).
- [38] K. P. Khemchandani, A. Martínez Torres, H. Nagahiro, and A. Hosaka, *Phys. Rev. D* **88**, 114016 (2013).
- [39] E. J. Garzon and E. Oset, *Phys. Rev. C* **91**, 025201 (2015).
- [40] J.-J. Xie, L.-R. Dai, and E. Oset, *Phys. Lett. B* **742**, 363 (2015).
- [41] X.-Z. Ling, M.-Z. Liu, J.-X. Lu, L.-S. Geng, and J.-J. Xie, *Phys. Rev. D* **103**, 116016 (2021).
- [42] J.-Y. Wang, M.-Y. Duan, G.-Y. Wang, D.-M. Li, L.-J. Liu, and E. Wang, *Phys. Lett. B* **821**, 136617 (2021).
- [43] R. Molina, J.-J. Xie, W.-H. Liang, L.-S. Geng, and E. Oset, *Phys. Lett. B* **803**, 135279 (2020).
- [44] M.-Y. Duan, J.-Y. Wang, G.-Y. Wang, E. Wang, and D.-M. Li, *Eur. Phys. J. C* **80**, 1041 (2020).
- [45] X. Zhu, H.-N. Wang, D.-M. Li, E. Wang, L.-S. Geng, and J.-J. Xie, *Phys. Rev. D* **107**, 034001 (2023).
- [46] J.-J. Xie and L.-S. Geng, *Eur. Phys. J. C* **76**, 496 (2016).
- [47] J.-J. Xie and L.-S. Geng, *Phys. Rev. D* **96**, 054009 (2017).
- [48] J.-J. Xie and L.-S. Geng, *Phys. Rev. D* **95**, 074024 (2017).
- [49] G.-Y. Wang, N.-C. Wei, H.-M. Yang, E. Wang, L.-S. Geng, and J.-J. Xie, *Phys. Rev. D* **106**, 056001 (2022).
- [50] R. Pavao, S. Sakai, and E. Oset, *Phys. Rev. C* **98**, 015201 (2018).
- [51] L.-L. Chau and H.-Y. Cheng, *Phys. Rev. D* **36**, 137 (1987); **39**, 2788(A) (1989).
- [52] L. L. Chau and H.-Y. Cheng, *Phys. Rev. D* **41**, 1510 (1990).
- [53] L.-L. Chau, H.-Y. Cheng, and B. Tseng, *Phys. Rev. D* **54**, 2132 (1996).
- [54] Q. Qin, J.-L. Qiu, and F.-S. Yu, *Eur. Phys. J. C* **83**, 227 (2023).
- [55] J. A. Oller, E. Oset, and J. R. Pelaez, *Phys. Rev. Lett.* **80**, 3452 (1998).
- [56] J. A. Oller, E. Oset, and J. R. Pelaez, *Phys. Rev. D* **59**, 074001 (1999); **60**, 099906(E) (1999); **75**, 099903(E) (2007).
- [57] E. J. Garzon and E. Oset, *J. Phys. Soc. Jpn. Conf. Proc.* **10**, 022004 (2016).
- [58] A. Ramos, E. Oset, and C. Bennhold, *Phys. Rev. Lett.* **89**, 252001 (2002).
- [59] P. Avery *et al.* (CLEO Collaboration), *Phys. Rev. Lett.* **71**, 2391 (1993).
- [60] M. Ablikim *et al.* (BESIII Collaboration), *Phys. Lett. B* **783**, 200 (2018).
- [61] M. Gronau, J. L. Rosner, and C. G. Wohl, *Phys. Rev. D* **97**, 116015 (2018); **98**, 073003(A) (2018).
- [62] X.-K. Dong, F.-K. Guo, and B.-S. Zou, *Phys. Rev. Lett.* **126**, 152001 (2021).
- [63] S. M. Flatte, *Phys. Lett. B* **63**, 224 (1976).
- [64] V. Baru, J. Haidenbauer, C. Hanhart, A. E. Kudryavtsev, and U.-G. Meissner, *Eur. Phys. J. A* **23**, 523 (2005).
- [65] J.-J. Xie, B.-C. Liu, and C.-S. An, *Phys. Rev. C* **88**, 015203 (2013).
- [66] M. Ablikim *et al.* (BESIII Collaboration), *J. High Energy Phys.* **09** (2023) 125.